JCI The Journal of Clinical Investigation

Resetting the transcription factor network reverses terminal chronic hepatic failure

Taichiro Nishikawa, … , Alejandro Soto-Gutierrez, Ira J. Fox

J Clin Invest. 2015;125(4):1533-1544. https://doi.org/10.1172/JCI73137.

Research Article **Hepatology**

The cause of organ failure is enigmatic for many degenerative diseases, including end-stage liver disease. Here, using a CCl_4-induced rat model of irreversible and fatal hepatic failure, which also exhibits terminal changes in the extracellular matrix, we demonstrated that chronic injury stably reprograms the critical balance of transcription factors and that diseased and dedifferentiated cells can be returned to normal function by re-expression of critical transcription factors, a process similar to the type of reprogramming that induces somatic cells to become pluripotent or to change their cell lineage. Forced re-expression of the transcription factor HNF4α induced expression of the other hepatocyte-expressed transcription factors; restored functionality in terminally diseased hepatocytes isolated from CCl_4-treated rats; and rapidly reversed fatal liver failure in CCl_4-treated animals by restoring diseased hepatocytes rather than replacing them with new hepatocytes or stem cells. Together, the results of our study indicate that disruption of the transcription factor network and cellular dedifferentiation likely mediate terminal liver failure and suggest reinstatement of this network has therapeutic potential for correcting organ failure without cell replacement.

Resetting the transcription factor network reverses terminal chronic hepatic failure

Taichiro Nishikawa,[1,2] Aaron Bell,[3,4] Jenna M. Brooks,[1] Kentaro Setoyama,[1] Marta Melis,[1] Bing Han,[1] Ken Fukumitsu,[3,4] Kan Handa,[3,4] Jianmin Tian,[3] Klaus H. Kaestner,[5] Yoram Vodovotz,[6] Joseph Locker,[3] Alejandro Soto-Gutierrez,[3,4] and Ira J. Fox[1]

[1]Department of Surgery, Children's Hospital of Pittsburgh of UPMC, and McGowan Institute for Regenerative Medicine, University of Pittsburgh, Pittsburgh, Pennsylvania, USA. [2]Department of Gastroenterology and Hepatology, Kyoto Prefectural University of Medicine, Kyoto, Japan. [3]Department of Pathology, University of Pittsburgh, Pittsburgh, Pennsylvania, USA. [4]McGowan Institute for Regenerative Medicine, Pittsburgh, Pennsylvania, USA. [5]Department of Genetics and Institute for Diabetes, Obesity and Metabolism, Perleman School of Medicine, University of Pennsylvania, Philadelphia, Pennsylvania, USA. [6]Department of Surgery, University of Pittsburgh and Center for Inflammation and Regenerative Modeling, McGowan Institute for Regenerative Medicine, Pittsburgh, Pennsylvania, USA.

The cause of organ failure is enigmatic for many degenerative diseases, including end-stage liver disease. Here, using a CCl_4-induced rat model of irreversible and fatal hepatic failure, which also exhibits terminal changes in the extracellular matrix, we demonstrated that chronic injury stably reprograms the critical balance of transcription factors and that diseased and dedifferentiated cells can be returned to normal function by re-expression of critical transcription factors, a process similar to the type of reprogramming that induces somatic cells to become pluripotent or to change their cell lineage. Forced re-expression of the transcription factor HNF4α induced expression of the other hepatocyte-expressed transcription factors; restored functionality in terminally diseased hepatocytes isolated from CCl_4-treated rats; and rapidly reversed fatal liver failure in CCl_4-treated animals by restoring diseased hepatocytes rather than replacing them with new hepatocytes or stem cells. Together, the results of our study indicate that disruption of the transcription factor network and cellular dedifferentiation likely mediate terminal liver failure and suggest reinstatement of this network has therapeutic potential for correcting organ failure without cell replacement.

Introduction

Cirrhosis of the liver, the final pathway for liver injury from multiple types of insults, is a process that is difficult to manage and is responsible for 1.2% of all US deaths (1). Late stages are characterized by portal hypertension, a terminal extrahepatic processes that result from fibrosis and vascular remodeling of the cirrhotic liver (2, 3), superimposed on liver failure, which results from the inability of hepatocytes to adequately synthesize coagulation factors, conjugate and secrete bilirubin, and regulate metabolism (4–7). Although some patients with advanced cirrhosis progress to terminal liver failure, others with the same histologic degree of cirrhosis develop less severe symptoms of hepatic dysfunction and survive. Aggressive management of portal hypertension and hepatic failure can extend life, but the only definitive therapy for end-stage cirrhosis is orthotopic liver transplantation (8).

The definitive cause of terminal organ failure in end-stage degenerative disease is poorly understood (2–8). With chronic injury, there is a decrease in hepatocyte mass, and the remaining hepatocytes have ongoing oxidative damage (9, 10), impaired mitochondrial function (11, 12), altered cellular energy production (13), telomere shortening (14, 15), and a decrease in regeneration capacity (13–15). Over the last decade, we developed a unique model in rats, using chronic administration of CCl_4 to produce a syndrome of progressive injury and irreversible and fatal chronic liver failure that greatly resembles human disease (13, 16). While the latter has different etiologies — including HBV, HCV, alcohol, or nonalcoholic steatohepatitis (NASH)/metabolic syndrome — this CCl_4-injured rat model reproduces the most important feature of advanced degenerative liver disease, the irreversibly decompensated hepatocyte. This rat model closely recapitulates the progressive liver failure that occurs in patients with Laennec's cirrhosis who have stopped alcohol consumption but still require transplantation to avoid succumbing to liver disease (Figure 1A).

Using this chronic injury model, we show that hepatocyte network transcription factors — HNF4α, FOXA2, C/EBPα, PPARα, and HNF1α — are stably downregulated in end-stage hepatocytes from animals with cirrhosis and terminal hepatic failure (13). Since recent studies have shown that somatic cells can be reprogrammed into pluripotent stem cells or other mature cell lineages following forced expression of selected transcription factors (17, 18), we examined whether reprogramming the disrupted transcription factor network in degenerative disease could reverse the acute decompensated and fatal organ failure mediated by chronic injury. We now report that forced re-expression of the transcription factor HNF4α can immediately revert senescent and irreversibly dysfunctional hepatocytes from terminal livers to normal function. Reprogramming the transcription factor network immediately corrected the phenotype of cultured end-stage cirrhotic hepatocytes and quickly reversed terminal end-stage liver failure in vivo without the need for regeneration through expansion of new hepatocytes or stem cells.

Conflict of interest: The authors have declared that no conflict of interest exists.
Submitted: October 22, 2014; **Accepted:** January 22, 2015.
Reference information: *J Clin Invest*. 2015;125(4):1533–1544. doi:10.1172/JCI73137.

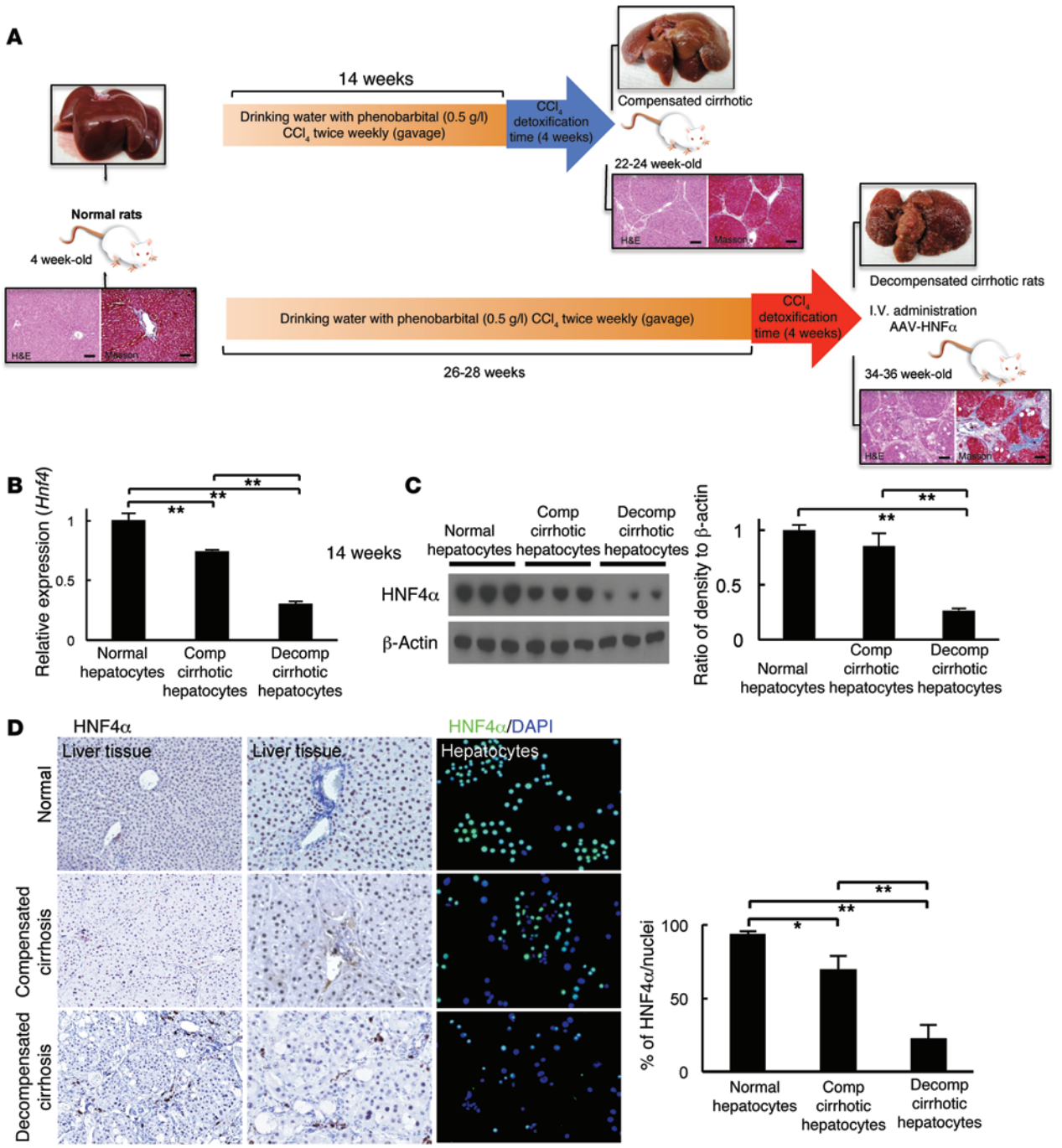

Figure 1. Schematic diagram for the induction of irreversible degenerative liver disease and terminal hepatic failure in rats and changes in HNF4α expression with disease progression. (**A**) Schematic diagram of the phenobarbital and CCl_4 treatment protocol. Scale bar: 100 μm. (**B**–**D**) Changes in HNF4α expression with disease progression. (**B**) qPCR and (**C**) Western blot for HNF4α expression in isolated hepatocytes from livers with degenerative disease and compensated (Comp) or decompensated (Decomp) function. (**D**) Immunohistochemistry of liver tissue and isolated hepatocytes; original magnification, ×100 and (cytospins) ×200. Normal age-matched livers or hepatocytes were used as controls. β-Actin was used as the PCR and Western blot control. qPCR and Western blot analysis were performed using three technical replicates and cDNA pooled from 4–5 animals per biological group. Immunohistochemistry is representative of four images per biologic group. Each value represents the mean ± SD (**B**–**D**). Statistical analyses were performed using the Tukey-Kramer multiple comparisons procedure among normal hepatocytes or compensated or decompensated cirrhotic hepatocytes (**B**–**D**, $*P < 0.05$, $**P < 0.01$).

Results

Chronic injury in terminal disease disrupts the hepatocyte-enriched transcription factor network, producing hepatocyte dedifferentiation and irreversible hepatic failure. Analysis of the transcriptome of hepatocytes recovered from rats with end-stage chronic liver disease showed that expression of *Hnf4a*, the central regulator of the adult hepatocyte transcription factor network, dramatically fell only with terminal loss of hepatic function (13). To confirm this finding, we performed a detailed analysis of the expression of HNF4α in isolated hepatocytes and liver tissue from animals with

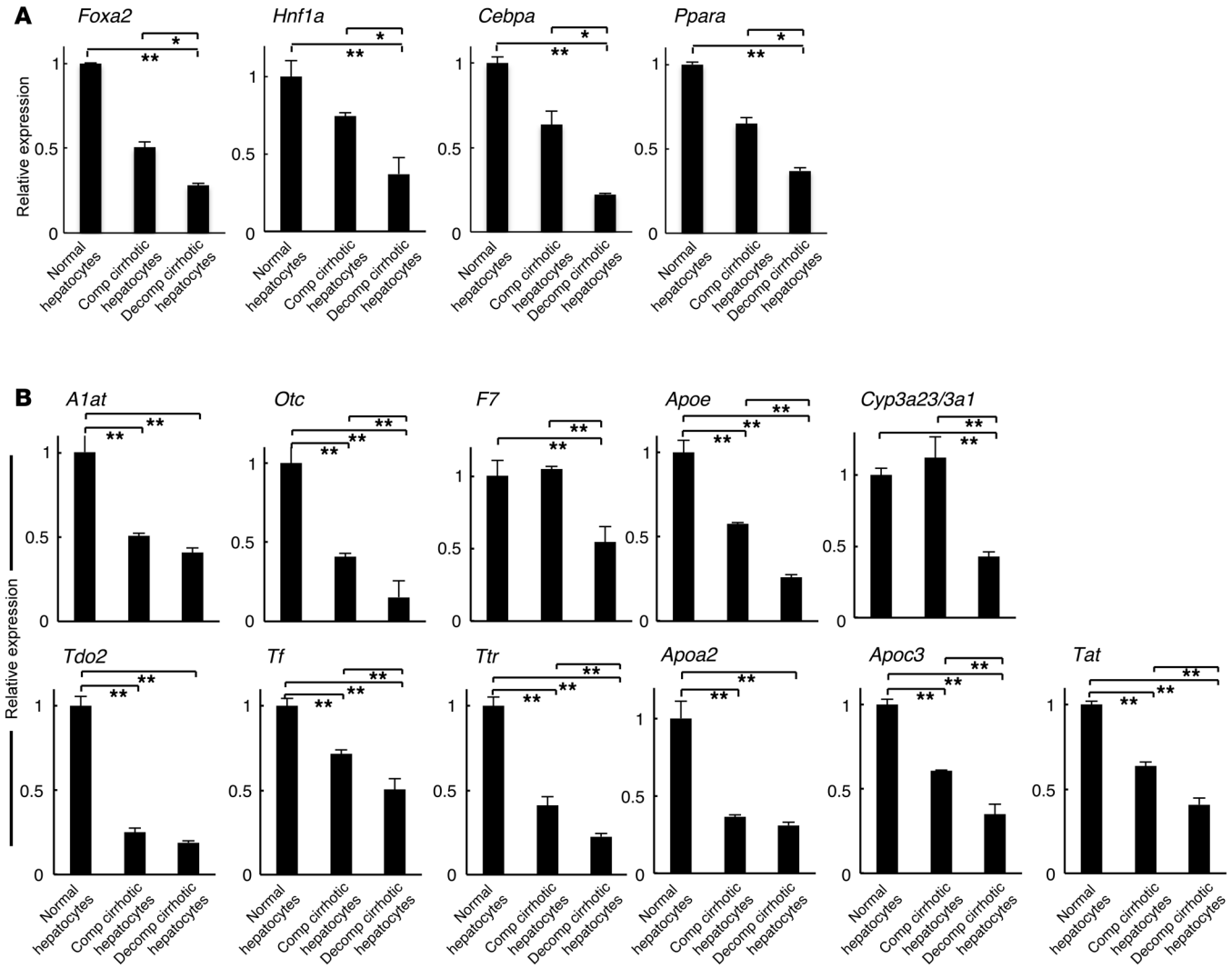

Figure 2. Hepatocyte-enriched transcription factor network genes and liver-specific genes are severely downregulated in decompensated hepatocytes from end-stage livers. (**A**) Expression changes by qPCR in the hepatocyte transcription factor network genes *Foxa2*, *Hnf1a*, *Cebpa*, and *Ppara* with progression from degenerative liver disease to chronic and terminal hepatic failure. (**B**) Expression of liver-specific genes and genes affected downstream of HNF4α. *A1at*, α1-antitrypsin; *Otc,* ornithine transcarbamylase; *F7*, coagulation factor VII; *Apoe*, *Apoa2*, and *Apoc3*, apolipoproteins E, A2, and C3; *Cyp3a23/3a1*, cytochrome P450 3a23; *Tdo2*, tryptophan 2,3-dioxygenase; *Tf,* transferrin; *Ttr*, transthyretin; and *Tat,* tyrosine aminotransferase. qPCR was performed using three technical replicates and cDNA pooled from 4–5 animals per biological group. Each value represents the mean ± SD (**A** and **B**). Statistical analyses were performed using the Tukey-Kramer multiple comparisons procedure among normal hepatocytes or compensated or decompensated cirrhotic hepatocytes (**A** and **B**, $*P < 0.05$, $**P < 0.01$).

chronic liver injury and fatal hepatic failure. Quantitative real-time PCR (qPCR) analysis demonstrated severe downregulation of *Hnf4a* expression, and quantification of HNF4α expression in hepatocytes by Western blot analysis and by immunofluorescence staining of cytospin samples gave similar results (Figure 1, B–D). Immunohistochemical localization of HNF4α showed expression in nuclei of hepatocytes but not in bile duct or other non-parenchymal cells. Nuclear HNF4α was present in the majority of hepatocytes from animals with compensated function but was severely diminished in hepatocytes in livers with terminal decompensated function. As downregulation of HNF4α expression has also been reported with hepatic dysfunction in human degenerative liver disease (19, 20), a significant decrease in HNF4α in hepatocytes appeared to correlate with end-stage chronic hepatic failure.

The possibility that transcription factor deficiency could explain hepatocyte impairment led us to perform a further analysis of microarrays. We found marked decreases in the expression not only HNF4α, but also FOXA2, C/EBPα, and HNF1α; these DNA-binding proteins are part of the network of hepatocyte-enriched transcription factors, sequentially established during development, that regulate the mature hepatocyte phenotype, controlling expression of proteins of coagulation, biliary metabolism, and lipid metabolism (13, 21, 22). We therefore assessed the expression of transcription factors *Foxa2*, *Cebpa*, *Ppara*, and *Hnf1a* by qPCR (Figure 2A). In addition, since HNF4α affects the expression of many liver-specific target genes involved in glucose, lipid, amino acid, xenobiotic, and drug metabolism (23), we also evaluated the expression of α1-antitrypsin; apolipoproteins A2, C3, and E;

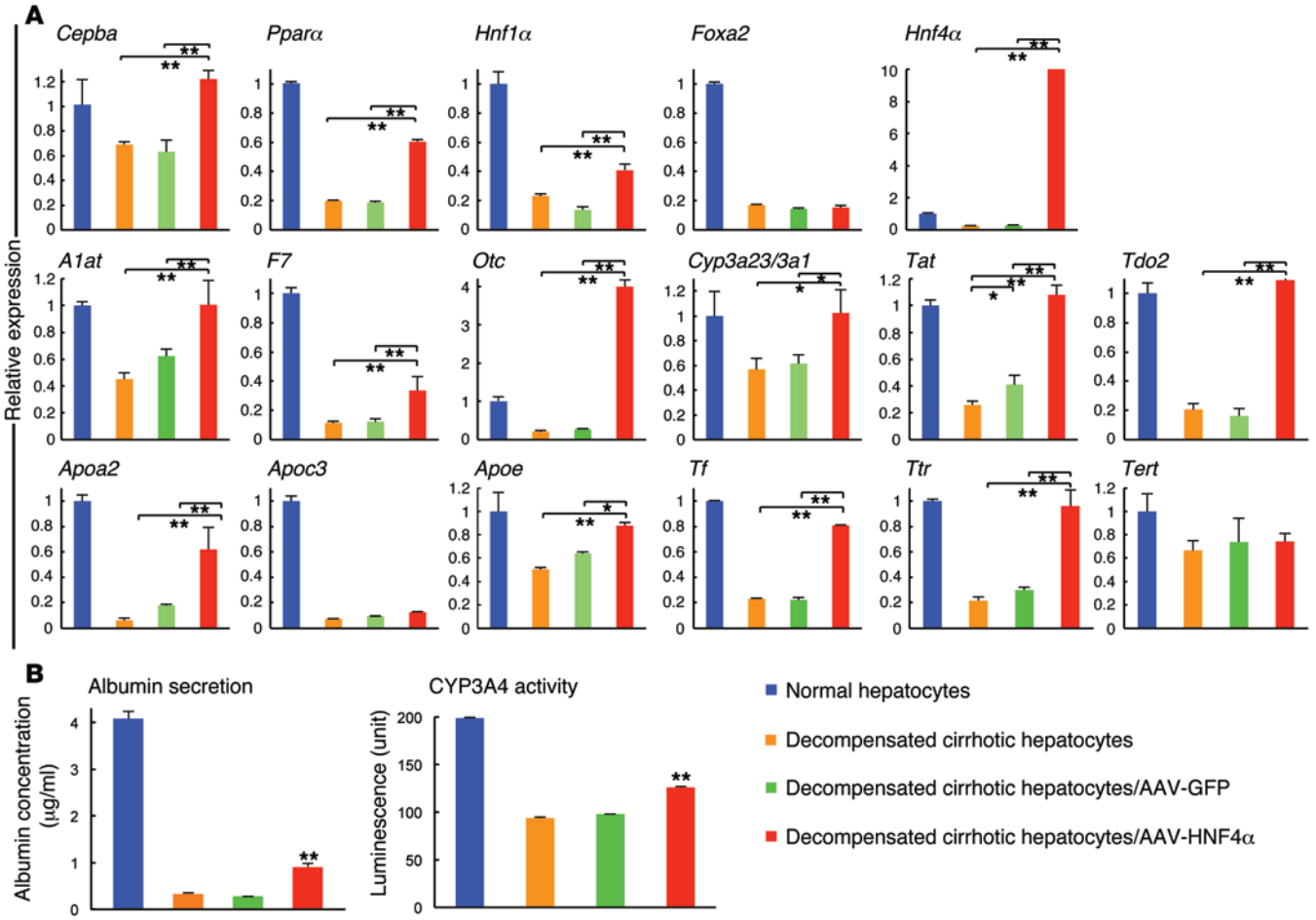

Figure 3. HNF4α re-expression in isolated hepatocytes from functionally decompensated livers with terminal cirrhosis shows immediate improvement in gene expression and function in vitro. (**A**) qPCR analysis of hepatocyte transcription factor network and hepatocyte-specific genes. (**B**) Albumin synthesis and cytochrome P450 (CYP3A4) activity. Studies were carried out on culture day 2 and compare hepatocytes from normal liver and decompensated cirrhotic livers, the latter also treated with AAV-HNF4α-GFP or AAV-GFP. Re-expression of HNF4α led to improvement in vitro within 48 hours. qPCR and albumin ELISA were performed using three technical replicates, and CYP activity was done using five technical replicates from hepatocytes isolated from one normal control and one decompensated cirrhotic animal. Each value represents the mean ± SD (**A** and **B**). Statistical analyses were performed using the Tukey-Kramer multiple comparisons procedure among normal hepatocytes and decompensated cirrhotic hepatocytes without and with AAV-HNF4α-GFP or AAV-GFP treatment. The statistical results are shown among decompensated cirrhotic hepatocytes without and with AAV-HNF4α-GFP or AAV-GFP treatment (**A**) and between decompensated cirrhotic hepatocytes without and with AAV-HNF4α-GFP (**B**) (*$P < 0.05$, **$P < 0.01$).

cytochrome P450 3a23, coagulation factor VII, ornithine transcarbamylase, tyrosine aminotransferase, tryptophan 2,3-dioxygenase, transferrin, and transthyretin. Indeed, all of the hepatocyte-enriched transcription factors and hepatocyte-specific genes were severely downregulated in terminal hepatic failure even 4 weeks after CCl_4 was discontinued (Figure 2, A and B).

Forced re-expression of HNF4α restores expression of hepatocyte-enriched transcription factors and reverses hepatocyte dedifferentiation in vitro. To test whether transcription factor deficiency could be responsible for impairment of hepatocyte function, we forced re-expression of HNF4α, one of the deficient factors, in chronic end-stage hepatocytes in vitro. Hepatocytes isolated from animals with fatal, irreversibly decompensated liver function were transduced in culture with adeno-associated virus (AAV) vectors to express HNF4α and GFP or GFP alone. At 48 hours, qPCR analysis showed HNF4α reprogramming restored to nearly normal levels the network transcription factors *Cebpa*, *Hnf1a*, and *Ppara* and the phenotypic target genes important for liver-specific activity (Figure 3A). Even within 48 hours, forced re-expression improved secretion of albumin — severely impaired in hepatocytes isolated from decompensated livers (13) — and cytochrome P450 activity, a major component of xenobiotic metabolism (Figure 3B).

HNF4α-mediated reprogramming immediately reverses liver failure in animals with end-stage degenerative disease. Our in vitro findings led us to examine whether transcription factor deficiency was responsible for fatal organ failure in animals with chronic end-stage liver disease. In previous studies of this model of chronic decompensated liver failure, we showed that intrasplenic hepatocyte transplantation improved liver function and survival, but was only effective for a period of weeks to months (16, 24) despite transplantation with syngeneic hepatocytes. Rats with chronic end-stage liver disease still died of progressive hepatic failure, and the severe changes in the extracellular matrix did not reverse after withdrawal of CCl_4. With this experimental background, we exam-

ined whether transcription factor reprogramming could reverse terminal liver failure in animals with end-stage disease by intravenous infusion of 3×10^{11} AAV-HNF4α-GFP virions. Costaining for GFP, albumin, α–smooth muscle actin (α-SMA), and EPCAM demonstrated that only albumin-positive hepatocytes were transduced. There was no evidence of non-parenchymal cell transduction (Figure 4A and Supplemental Figure 1; supplemental material available online with this article; doi:10.1172/JCI73137DS1).

Impaired albumin expression by immunofluorescence was dramatically improved by re-expression of HNF4α (Figure 4B), and pathophysiologic testing showed striking and persistent improvement in liver function, activity, and neurologic function. Survival was also prolonged to the end point of the study at 100 days following AAV treatment (Figure 4C). Administration of the AAV-GFP control vector did not affect liver function or survival. Functional analysis of cells isolated from HNF4α-treated animals showed significant improvement of albumin secretion, CYP450 activity (Figure 5A), and expression levels of HNF4α target genes (Figure 5B). These data were confirmed by RNA-Seq analysis (Supplemental Figure 2).

Hepatic failure is reversed by phenotypically correcting diseased hepatocytes, not by regeneration through stem cells or new hepatocytes. The healing effects of hepatocyte reprogramming did not depend on proliferation, since there was no increase in Ki-67 staining (Figure 6A). As expected, hepatocyte apoptosis was prominent in decompensated livers, as assessed by TUNEL staining, but apoptotic cell death was significantly reduced following HNF4α reprogramming (Supplemental Figure 3, A and B), and there was a decrease in expression of the hepatic progenitor cell markers *Afp*, *Cd44*, and *Epcam* (Figure 6B), suggesting that cell survival was improved by reprogramming. Thus, expansion of adult hepatocytes or stem cells played no role in recovery. We further examined whether hepatocytes recovered from animals with terminal hepatic failure that were previously treated with HNF4α could expand when transplanted into host livers in which there was a repopulation advantage to donor over host hepatocytes (13). HNF4α-treated end-stage hepatocytes were unable to expand in the livers of Nagase analbunemic host rats to any significant extent (Supplemental Figure 4), and this is reflected by limited production of serum albumin in recipient rats by transplanted hepatocytes that generate albumin at normal levels (Figure 6C). HNF4α-mediated reprogramming also did not significantly augment *Tert* expression or telomere length, which remained critically short, in hepatocytes derived from failed livers (Figure 6D). Thus, HNF4α acted by phenotypically correcting diseased hepatocytes, not by stimulating their replacement.

Discussion

Our results show that the hepatocyte in fatal end-stage liver disease has a new stable phenotype — in the intact liver and in cell culture — that does not reverse despite elimination of the cause of injury. This new phenotype reflects disruption of the transcription factor network through downregulation of the major hepatocyte-enriched transcription factors. Thus, stable downregulation of the transcription factor network is responsible for hepatocyte dedifferentiation and hepatic failure in terminal chronic degenerative liver disease. Replenishment of HNF4α rapidly revitalized expression of the other hepatocyte-enriched transcription factors and normalized hepatocyte function in vitro, while reprogramming hepatocytes in animals with degenerative liver disease and irreversibly decompensated function produced a profound and rapid improvement in liver function. The failing hepatocyte did not have to be replaced through regeneration by stem cells or new hepatocytes, and the matrix did not have to get repaired for the hepatocytes to be completely corrected; resolution of hepatic failure required only restoration of the transcription program. The outcome is a striking demonstration of the central role of HNF4α within the hepatocyte transcription factor network (21, 25, 26).

Although HNF4α may not be unique in its ability to correct the disrupted transcription network, it was effective in our experiments. Impaired expression of HNF4α could reflect direct regulation or inhibition of another network factor that activates HNF4α transcription (27–29) and could result from either cell-extrinsic or cell-intrinsic mechanisms. Toxins, chemical injury, and cytokines generated from inflammation or injured cells can all induce inhibition of critical transcription factors (30). Such extrinsic mechanisms should be corrected immediately by removing the injury in vivo, or by culturing the hepatocytes in vitro. However, neither withdrawing CCl_4 nor placing hepatocytes from end-stage cirrhotic livers in culture effectively reversed the hepatocyte dysfunction. Since downregulation of the network factors HNF1α, FOXA2, CEBPα, and PPARα was also clear in our studies, it is likely that *Hnf4a*, or another network gene, is the critical target of an inhibitory pathway.

The precise molecular details responsible for this disruption will require further study. Research on hepatocyte injury has highlighted three candidate pathways that could mediate this inhibition — TNF-α/NF-κB, IL-6/STAT3, and TGF-β/SMAD — and our prior research showed NF-κB and TGF-β signatures by microarray and direct transcript analysis (31). Thus, it is likely that cytokine/injury effects alter expression of the hepatocyte transcription factor network by extrinsic mechanisms, with the result that network factors establish a new steady-state equilibrium in the dysfunctional hepatocyte that can no longer compensate to restore normal gene expression. In our studies reprogramming the liver-enriched transcription factor network by HNF4α treatment did not require prolonged expression of virus-mediated HNF4α. Fourteen weeks after intervention, essentially all HNF4α expression was mediated by the endogenous gene, and AAV-HNF4–specific transcripts were expressed at extremely low levels (Supplemental Figure 5, A and B). This lack of necessity for prolonged expression of exogenous reprogramming genes is similar to that seen following reprogramming somatic cells to pluripotency (17, 18). HNF4α is an essential transcription factor during embryonic development, and its expression continues in the adult liver and in other extrahepatic tissues. Since we did not examine whether AAV intervention resulted in enhanced extrahepatic HNF4α expression, we cannot rule out an independent effect on a small number progenitor cells, but the restoration of the liver phenotype must occur by reprogramming and correction of hepatocytes.

The mechanism by which HNF4α re-expression corrects individual hepatocyte dysfunction is delineated by in vitro studies, where reactivation of a range of HNF4α target genes, including the transcription factors, serum proteins, coagulation factors,

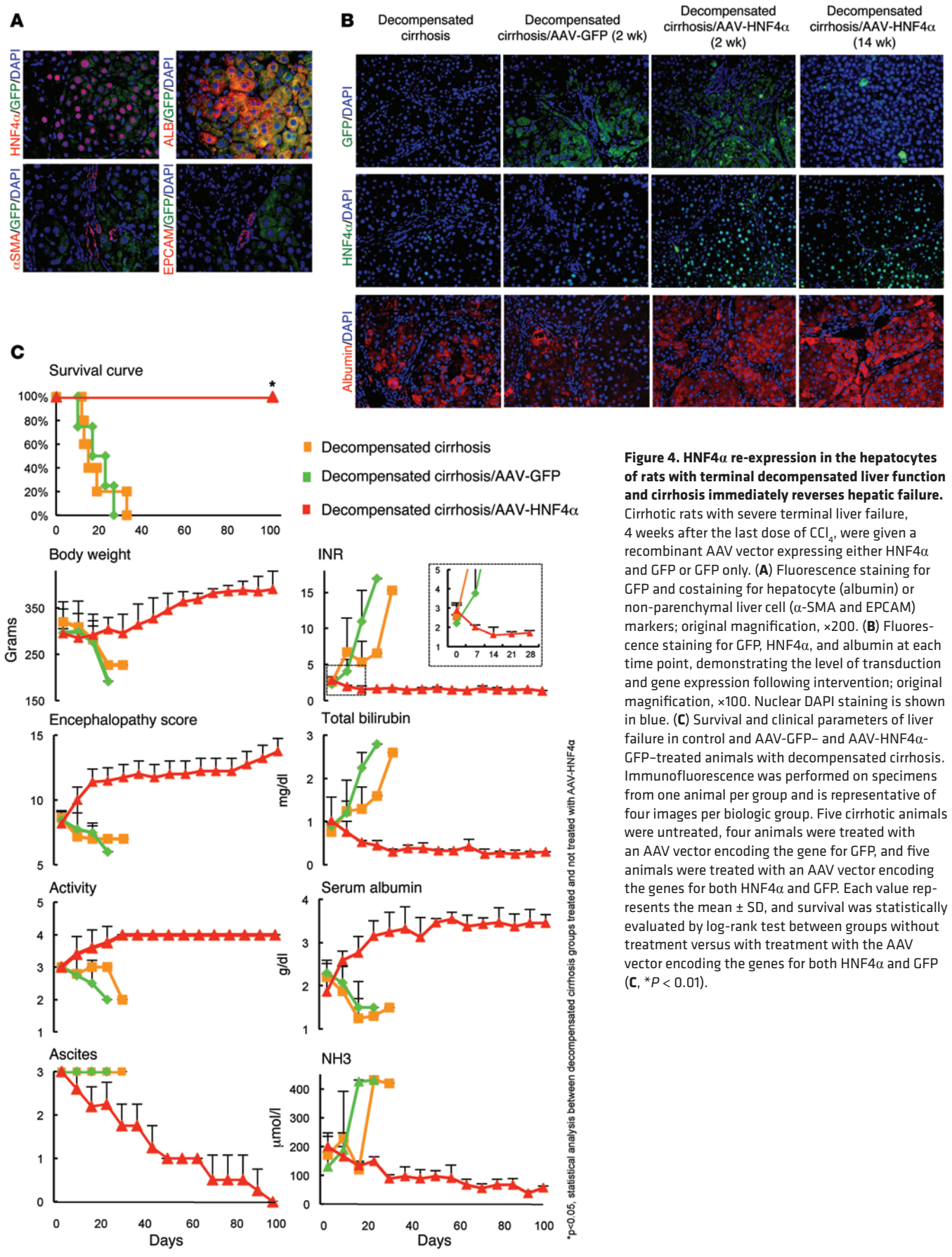

Figure 4. HNF4α re-expression in the hepatocytes of rats with terminal decompensated liver function and cirrhosis immediately reverses hepatic failure. Cirrhotic rats with severe terminal liver failure, 4 weeks after the last dose of CCl_4, were given a recombinant AAV vector expressing either HNF4α and GFP or GFP only. (**A**) Fluorescence staining for GFP and costaining for hepatocyte (albumin) or non-parenchymal liver cell (α-SMA and EPCAM) markers; original magnification, ×200. (**B**) Fluorescence staining for GFP, HNF4α, and albumin at each time point, demonstrating the level of transduction and gene expression following intervention; original magnification, ×100. Nuclear DAPI staining is shown in blue. (**C**) Survival and clinical parameters of liver failure in control and AAV-GFP– and AAV-HNF4α-GFP–treated animals with decompensated cirrhosis. Immunofluorescence was performed on specimens from one animal per group and is representative of four images per biologic group. Five cirrhotic animals were untreated, four animals were treated with an AAV vector encoding the gene for GFP, and five animals were treated with an AAV vector encoding the genes for both HNF4α and GFP. Each value represents the mean ± SD, and survival was statistically evaluated by log-rank test between groups without treatment versus with treatment with the AAV vector encoding the genes for both HNF4α and GFP (**C**, $*P < 0.01$).

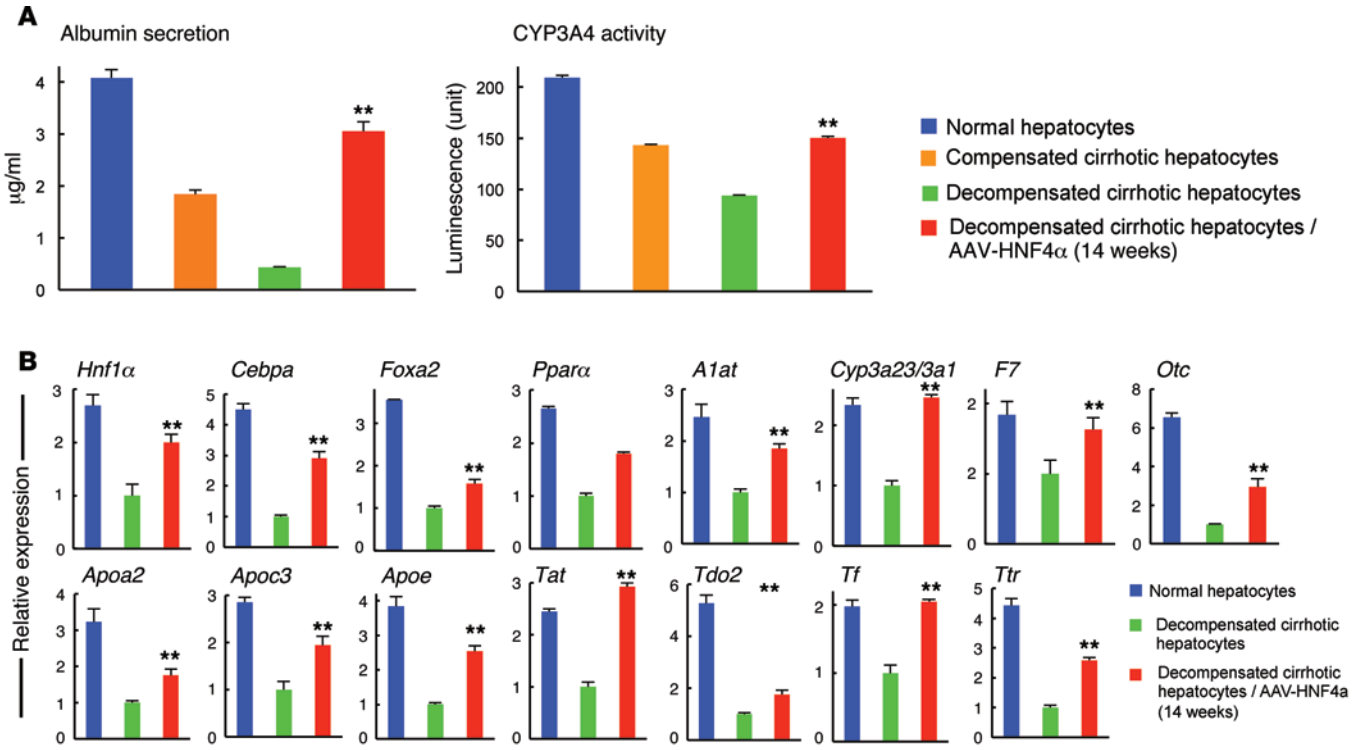

Figure 5. Hepatocytes recovered from treated rats with terminally decompensated function and cirrhosis after HNF4α re-expression show normalization of function and gene expression profile. (**A**) Albumin synthesis and cytochrome P450 (CYP3A4) activity in decompensated hepatocytes recovered 14 weeks after AAV-HNF4α/GFP treatment. Hepatocytes recovered from normal livers and cirrhotic livers with normal liver function were used as controls. (**B**) qPCR analysis of hepatocyte transcription factor network and hepatocyte-specific gene expression in age-matched control hepatocytes and hepatocytes recovered from functionally decompensated livers and decompensated cirrhotic livers 14 weeks after AAV-HNF4α/GFP treatment. Studies were performed using three technical replicates from hepatocytes isolated from one animal representing each biological group. Each value represents the mean ± SD. Statistical analyses were performed using the Tukey-Kramer multiple comparisons procedure among isolated hepatocytes from normal livers and compensated and decompensated cirrhotic livers and decompensated cirrhotic livers 14 weeks after AAV-HNF4α/GFP treatment. Significant differences are shown between cells from decompensated cirrhotic livers and decompensated cirrhotic livers 14 weeks after AAV-HNF4α/GFP treatment (**A** and **B**, $^{**}P < 0.01$).

and metabolic enzymes critical for hepatic function, takes place within 48 hours of transduction, a common time sequence for this type of transcriptional effect. HNF4α therapy directly reverses the deteriorating hepatic function responsible for the complications of hepatocyte failure — i.e., worsening coagulopathy, worsening encephalopathy, increased ammonia levels, decreased serum colloid, ascites, and cachexia — that result in death in untreated rats.

While the AAV promoter used is nonspecific, AAV has a strong tropism for hepatocytes (32), and the DJ serotype has been optimized for hepatocyte-mediated gene therapy (33). Furthermore, following transduction, exogenous *Hnf4a* gene expression was at only a fraction of the endogenous level. Thus, any non-parenchymal cell contribution would be limited, and our double-staining immunofluorescence studies support this finding. Moreover, HNF4α expression both before and following treatment was confined to hepatocytes. Thus, restoration of damaged hepatocytes appears to be the dominant mechanism responsible for starting this process.

As noted, long-term correction took place despite the fact that forced re-expression generated only 0.01% of the endogenous level of HNF4α. To explain this, it is important to remember that HNF4α is the central member of a network of mutually regulated hepatocyte transcription factors. These are all downregulated in failure, and HNF4α reawakens the entire network. Thus, HNF4α upregulates the downstream transcription factors HNF1α, PPARα, C/EBPα, and FOXA2, which, in turn, upregulate endogenous HNF4α, as well as each of the other network transcription factors. This reciprocal support appears to result in sustained correction of the endogenous transcription factor network and of the phenotype.

Our data show that only a modest fraction of hepatocytes are transduced. We did not perform a dose response study, so the minimum number of transduced hepatocytes required for correction of liver failure is unclear from the current study. However, we previously demonstrated that splenic engraftment of approximately 3% of hepatocyte mass of the liver partially corrects the failure phenotype, but not portal hypertension, in this model of chronic liver failure from cirrhosis (16). Thus, partial correction of hepatic functional decompensation may only require intact function of a relatively modest number of hepatocytes in end-stage degenerative disease.

This initial phenotypic correction is certainly part of the story. However, at 14 weeks complete normalization of hepatic function was shown. Thus, additional hepatocytes undergo correction over time from an additional process. The interaction between the extracellular matrix and the hepatocytes within that matrix is a dynamic process. Whether correction of untrans-

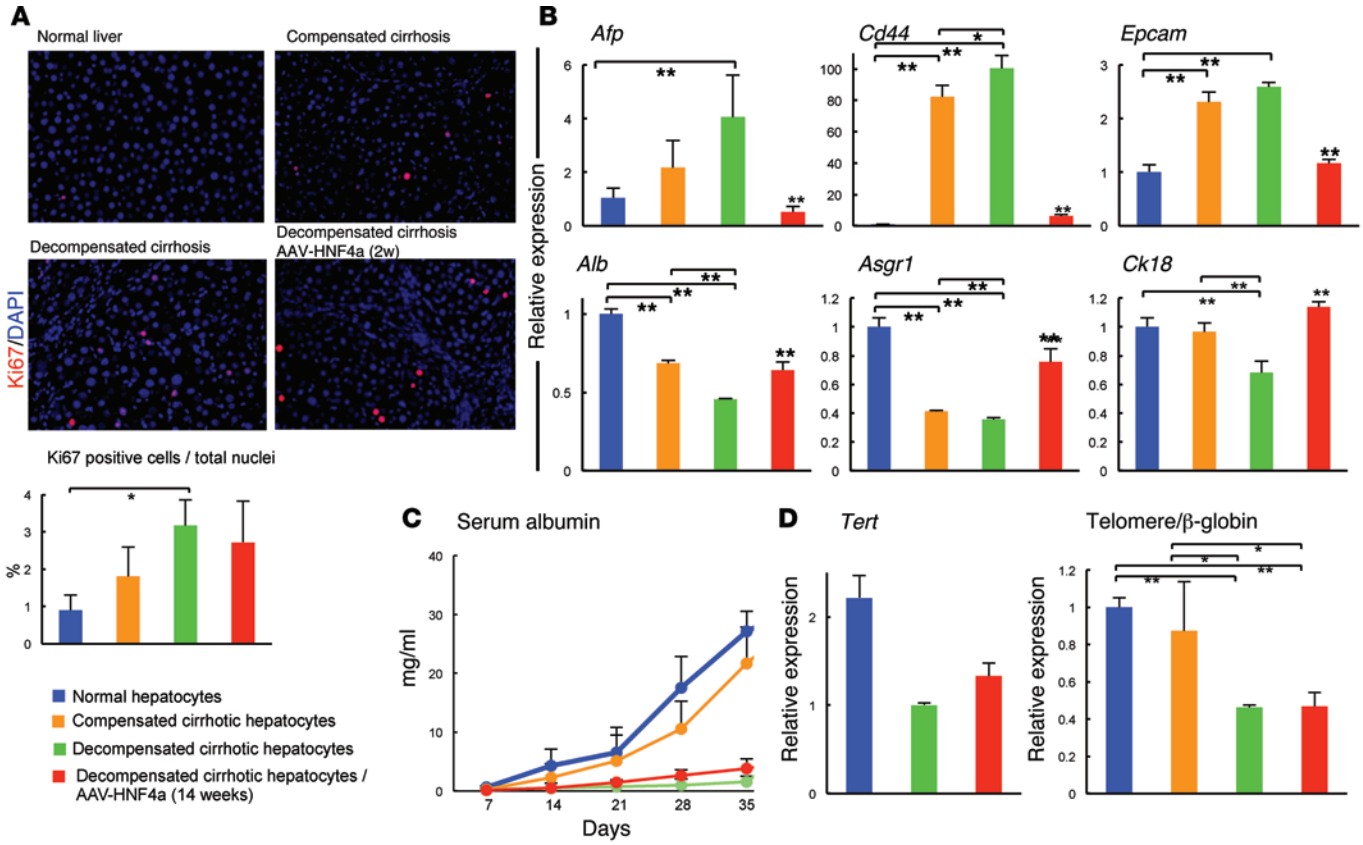

Figure 6. Improvement in liver function after treatment with HNF4α re-expression is not mediated by expansion of new cells. (**A**) Fluorescence staining for Ki-67, a proliferation marker in AAV-HNF4α-GFP–treated decompensated cirrhotic hepatocytes; original magnification, ×200. Images are representative of four images per biologic group. (**B**) qPCR analyses of hepatic progenitor marker genes (*Afp*, *Cd44*, and *Epcam*) and mature hepatic-specific genes (*Alb*, *Asgpr1*, and *Ck18*) from animals with liver disease. (**C**) HNF4α-treated end-stage hepatocytes were transplanted into the livers of Nagase analbuminemic rats, which were treated with retrorsine and underwent partial hepatectomy. (**D**) qPCR analysis for *Tert* expression and telomere length by genomic DNA analysis. qPCR and other studies were performed using three technical replicates from hepatocytes isolated from one animal representing each biological group. Each transplant group represents five animals infused with hepatocytes isolated from one animal that underwent each of the various interventions. Each value represents the mean ± SD (**A**–**D**). Statistical analyses were performed using the Tukey-Kramer multiple comparisons procedure among isolated hepatocytes from normal livers, compensated and decompensated cirrhotic livers, and decompensated cirrhotic livers 14 weeks after AAV-HNF4α/GFP treatment. Statistical results are shown among three groups (normal hepatocytes and functionally compensated and decompensated hepatocytes from cirrhotic livers) and between untreated decompensated cirrhotic hepatocytes and decompensated cirrhotic hepatocytes 14 weeks after in vivo HNF4α re-expression (**A** and **B**, $*P < 0.05$, $**P < 0.01$); and among isolated hepatocytes from normal livers, compensated and decompensated cirrhotic livers, and decompensated cirrhotic livers 14 weeks after AAV-HNF4α/GFP treatment (**D**, $*P < 0.05$, $**P < 0.01$).

duced hepatocytes takes place through cell-cell communication, or elaboration of paracrine mediators that also modulate the extrahepatic environment, which in turn correct hepatocyte phenotype, is an intriguing question that will require extensive additional work.

The concept that restoration of normal function in degenerative liver disease requires replacing diseased hepatocytes through expansion of mature hepatocytes or differentiation and expansion of induced progenitors is prevalent in therapeutic research. Instead, we show a more expedient strategy, direct transcriptional reprograming of terminally diseased hepatocytes in situ, a strategy that works even without correcting senescence. Although forced re-expression of HNF4α in the liver has been previously shown to reverse hepatic fibrosis (34), we have demonstrated that improvement in hepatic function begins within 48 hours of HNF4α re-expression. Our studies show that reversal of the distorted extracellular matrix is not absolutely required to reverse hepatic failure in degenerative liver disease, as only minimal resolution of fibrosis was found by histology 2 weeks after forced re-expression of HNF4α, well after improvement in hepatic function was documented (Supplemental Figure 6, A and B). Significant improvement in histology, however, was observed at 100 days. These findings are in sharp contrast to our previously published results showing that hepatocyte transplantation does not resolve fibrosis (16, 24). A comparable strategy with an appropriate transcription factor might restore loss of function in other chronic diseases (35, 36), even when advanced changes in the extracellular matrix are present.

Methods

Animals. Lewis rats were obtained from Charles River and were maintained in isolation cages in the Department of Laboratory and Animal Resources at the University of Pittsburgh. Animals were housed in temperature- and light/dark cycle–controlled rooms.

Induction of liver cirrhosis. Liver cirrhosis was induced as described previously by using phenobarbital and CCl_4 (both Sigma-Aldrich) when inbred male Lewis rats, weighing 100–130 g, were 4 weeks old (16). Rats were given phenobarbital (0.5 g/l) added to the drinking water. Starting 2 weeks later, CCl_4 (diluted 1:9 in olive oil) was administered by gavage twice a week. Following an initial dose of 0.2 ml/kg, each subsequent dose was adjusted weekly on the basis of changes in body weight. If body weight increased or remained unchanged, CCl_4 was continued at 0.2 ml/kg twice weekly. When body weight decreased by 1–5 g, the dose of CCl_4 was reduced to 0.15 ml/kg, and if body weight decreased by 6–10 g, the CCl_4 was reduced to 0.1 ml/kg. In rats that lost more than 10 g of body weight, CCl_4 was withheld until reassessment 1 week later. All animals were monitored for body weight, activity, and amount of ascites; and by hepatic encephalopathy (HE) score, which constituted a coma scale based on spontaneous levels of flexion, grasping, righting, placement, and corneal and head-shaking reflexes. Normal activity score was 5; maximum ascites score was 3; and an HE score of 15 indicated normal behavior (37). Activity was measured on a 5-point scale, with 5 representing normal activity; 4, some decrease in walking and running; 3, lethargy; 2, no spontaneous movement unless stimulated; and 1, no spontaneous movement. Ascites was assessed on a scale from 0 to 3 based on visual inspection. Absence of ascites was recorded as 0; barely palpable ascites, 1+; gross ascites with expansion of the flanks, 2+; and tense ascites, 3+. Whole blood was obtained at different time points and analyzed for bilirubin and albumin using a microfluidic metabolic assay system (Piccolo-Abaxis). Ammonia (NH_3) and international normalized ratio (INR) in serum were measured in the clinical laboratory at the Children's Hospital of Pittsburgh.

When rats received a minimum of 2.6 ml CCl_4 and developed persistent ascites, an activity score of <4, and an HE score of <10, laboratory tests were performed weekly to estimate liver function. Phenobarbital and CCl_4 were discontinued when (a) plasma total bilirubin levels exceeded 0.5 mg/dl (normal <0.2 mg/dl); (b) the INR exceeded 1.7; (c) plasma ammonia concentrations were above 90 mmol/l (normal <70 mmol/l); (d) ascites was found to be persistent by clinical examination; and (e) the HE score was persistently <10. If 4 weeks after complete cessation of phenobarbital and carbon tetrachloride treatment the laboratory measures, encephalopathy score, and ascites did not improve, rats were considered to have chronic liver failure from decompensated cirrhosis. All animals receiving CCl_4 were observed for 4 weeks after receiving their last dose of CCl_4 to eliminate the acute effects of toxin exposure before hepatocytes were recovered for analysis and transplantation.

Animals required 2.8 ± 0.2 ml CCl_4 over 26–28 weeks to generate cirrhosis that produced irreversible liver failure, and these animals died approximately 2–4 weeks after the 4-week observation period, with progressive worsening of liver function if they received no treatment. Animals with cirrhosis without liver failure received 13–14 weeks of CCl_4 and a total dose of 1.3 ± 0.1 ml of CCl_4. Laboratory tests and ascites resolved quickly in all of these animals after the 4-week observation period after discontinuation of carbon tetrachloride.

Isolation of hepatocytes. Hepatocytes were isolated from donor rats by in situ collagenase perfusion as originally described by Berry and Friend and later modified by Seglen (38, 39). The perfusion time varied from 10 to 20 minutes based on the consistency of liver tissue in response to collagenase digestion. Cell viability, as assessed by trypan blue exclusion and by plating efficiency at 24 hours, was required to be 80% or greater to be acceptable for in vitro analysis. For cytospin samples, 5×10^4 hepatocytes were centrifuged at 50 *g* for 5 minutes for attachment to slides. After air drying, the cells were fixed with 4% paraformaldehyde for 15 minutes and preserved at –80°C.

Hepatocyte culture. Five hundred thousand hepatocytes isolated from control and cirrhotic livers were seeded into individual wells of collagen-coated 6-well plates (BD) and cultured at 37° in 5% CO_2 in F-12 medium (DMEM supplemented with 5% FBS, 2 mM glutamine, 100 U/ml penicillin, 100 μg/ml streptomycin, 100 nM dexamethasone, 0.872 μM insulin, and 5 ng/ml epithelial growth factor). Tissue culture medium was changed after overnight culture following the isolation and freshly exchanged everyday. The supernatant was collected 24 hours later to determine albumin secretion.

Total RNA extraction and qPCR. RNA was extracted from isolated rat hepatocytes or liver tissue using the RNeasy Mini Kit (QIAGEN) according to the manufacturer's instructions. RNA quantity and integrity were evaluated using a NanoDrop 1000 spectrometer (Thermo Fisher Scientific Inc.). cDNA was reverse transcribed from 1 μg total RNA using SuperScript III reverse transcriptase (Invitrogen). For endogenous HNF4α and AAV-specific HNF4α expression studies, reactions were performed on 96-well plates using a TaqMan RT-PCR Master Mix Reagent kit (Applied Biosystems) in a total volume of 20 μl consisting of 3 mM $MgCl_2$, 0.2 mM/each dNTP, 200 nM TaqMan probe, primers, and 1.25 U AmpliTaq Gold (Life Technologies). The TaqMan probes consisted of an oligonucleotide with a 5′ reporter dye (FAM) and a downstream 3′ quencher dye (NFQ) (endogenous HNF4α ID: AIFAS6FRHNG4A.1545S.1; AAV-specific HNF4α ID: AIPAEINRHNF4.1390S.1). For other studies, gene expression was measured using Power SYBR Green PCR Master Mix (Applied Biosystems), using an ABI 7500 Real-Rime PCR System. The sequences of the primers used for this study are listed in Supplemental Table 1. The PCR reaction was programmed as follows: initial denaturing at 95°C for 10 minutes, followed by 95°C for 15 seconds, 60°C for 1 minute, cycled 40 times. The median cycle threshold value and the relative cycle threshold method were used for analysis. All cycle threshold values were normalized to the expression of the housekeeping gene *Actb*. All reactions were performed with four biological replicates and three technical replicates with reference dye normalization. All values were normalized to control normal hepatocytes. A *P* value of less than 0.05 was used for the significance cutoff point for all genes tested. ANOVA (Tukey-Kramer multiple comparison test) was used for statistical comparison within experimental groups. Each value represents the mean ± SD.

RNA-seq. Total RNA was extracted from whole liver tissue using the miRNeasy Mini Kit (QIAGEN), followed by ribosomal RNA depletion using the RiboMinus Eukaryotic System V2 (Life Technology). Following generation of cDNA libraries (http://wasp.einstein.yu.edu/index.php/Protocol:RNA_seq), indexed sequencing libraries were generated using a TruSeq Nano DNA Sample Preparation kit (Illumina). 100-bp paired-end sequencing was carried out using an Illumina HiSeq 2500 instrument, and the sequence reads were aligned against the rat genome (rn5) using TopHat (40). One library from each experimental group was also aligned to the AAV-GFP-HNF4α viral construct. Aligned output from each library was visualized with GenPlay software (http://www.genplay.net) (41). In this software platform, transcripts were quantified by scoring exons with a base coverage sum algorithm, and then output scores for each library were normalized using the values obtained for *Gapdh*.

DNA extraction and telomere length measurement by qPCR. Genomic DNA was extracted from isolated rat hepatocytes and used for examination of telomere length in qPCR using the modified Cawthon's method (42). The telomere/single copy gene (T/S) ratio was calculated as the index of telomere length in each sample. Triplicate PCR reactions for each sample were performed with Power SYBR Green PCR Master Mix, DNA, and primer pairs using the ABI 7500 Real-Time PCR System. Primers for telomeres and β-globin were added to a final concentration of 250 nM. The primer sequences were tel-1, 5′-GGTTTTTGAGGGTGAGGGTGAGGGTGAGGGTGAGGGT-3′; tel-2, 5′-TCCCGACTATCCCTATCCCTATCCCTATCCCTATCCCTATCCCTA-3′; β-globin-F, 5′-CAGCAAGTGGGAAGGTGTAATCC-3′; β-globin-R, 5′-CCCATTCTATCATCAACGGGTACAA-3′. Standard curves for both telomere length and the single copy gene were generated from five concentrations (42, 25.2, 15.1, 9.1, 5.4 ng/aliquot) of a reference DNA sample serially diluted 1.68-fold with PCR grade water.

Western blot analysis. Isolated hepatocyte fractions were lysed in RIPA buffer (Sigma-Aldrich) with 1% proteinase inhibitor cocktail (Calbiochem) on ice. Forty micrograms of the cellular protein was electrophoresed in a 4%–12% Bis-Tris gel and then transferred to a nitrocellulose membrane (Invitrogen). Antibodies for HNF4α and β-actin were purchased from Abcam and Cell Signaling Technology, respectively.

Histology. Five-micrometer-thick sections were prepared from paraffin-embedded liver tissue fixed in 4% paraformaldehyde (PFA), and two slides each were used for H&E and Masson trichrome staining according to the manufacturer's protocols (Sigma-Aldrich).

Immunohistochemistry. Sections, 5 μm in thickness, were heated in a microwave oven in citrate sodium buffer, pH 6.0 (Dako), for 5–10 minutes at 95°C and cooled at room temperature for 20 minutes. After blocking with PBS and 2% FCS for 15 minutes, samples were incubated with one or a combination of diluted primary antibodies (1:100) for 1 hour at room temperature. After washing 3 times in PBS, samples were incubated with diluted secondary antibodies conjugated with fluorochromogen (1:250) for 60 minutes at room temperature for immunofluorescence staining. Samples were then mounted in VECTASHIELD (Vector Laboratories) containing DAPI solution. Immunohistochemistry was also performed using the same method described above, except for the blocking of endogenous peroxidase by incubation in methanol and 0.3% hydroxyperoxidase for 20 minutes. The VECTASTAIN ABC kit for mouse IgG (Vector Laboratories) was used to detect the immunocomplex signal, and the samples were counterstained using Gill's hematoxylin for 60 seconds. The stained samples were examined using an Olympus Provis light microscope. TUNEL staining was done using a commercially available kit (DeadEnd Colorimetric TUNEL System) following the manufacturer's instructions (Promega; G7130 and G7360). Mouse anti-HNF4α monoclonal antibody, rabbit anti-GFP polyclonal antibody, rabbit anti-EPCAM polyclonal antibody, rabbit Ki-67 polyclonal antibody, and mouse anti–α-SMA monoclonal antibody were purchased from Abcam; mouse anti-GFP monoclonal antibody from Cell Signaling Technology; and sheep anti–rat albumin polyclonal antibody from Bethyl Laboratories Inc. as primary antibodies in this study (catalog numbers are provided in Supplemental Table 2). Alexa Fluor 488–conjugated goat anti-rabbit IgG and anti-mouse IgG antibodies and Alexa Fluor 594–conjugated goat anti-rabbit IgG, anti-mouse IgG, and donkey anti-sheep IgG antibody were purchased from Invitrogen as secondary antibodies. For calculation of percent positive cells, at least four low-power digital images (×100) per sample were analyzed using an Olympus Provis light microscope using ImageJ software (http://imagej.nih.gov/ij/).

AAV cloning and virus preparation. Two AAV vectors, serotype AAV-DJ, were used for these studies: one capable of transferring GFP, pAAV-GFP; and the other capable of expressing HNF4α and GFP, pAAV-HNF4α/GFP, which expresses both HNF4α and GFP in a single transcription unit under control of the CMV promoter. Cells were transduced in vitro at an MOI of 2,000, and the transduction efficiency in vitro was >90%.

A 1.5-kb EcoRI fragment of rat *Hnf4a* 2 (NM 022180.2) was cloned into the bicistronic plasmid pAAV-IRES-GFP (Cell Biolabs Inc.), which expresses *Hnf4a* under control of the CMV promoter and GFP under control of the IRES. AAV vector preparation was performed using the helper virus–free $CaPO_4$ triple transfection method. Supernatant was collected, and virus was purified and concentrated using the ViraBind AAV purification kit (Cell Biolabs Inc.) per the manufacturer's instructions. Viral titer in genome copies (gc)/ml was determined by dot blot of serial dilutions of virus using linearized pAAV-CMV-HNF4α/IRES-GFP as a standard and an HNF4α cDNA fragment as probe.

Transduction to express HNF4α. For in vitro studies, freshly isolated hepatocytes were plated at a density of 0.5 million cells per well in collagen-coated 6-well plates. After incubation in DMEM/F12 for 2 hours at 37°C and 5% CO_2, the culture medium was changed to one containing each AAV vector at an MOI of 2,000. Cells were incubated for 24 hours at 37°C and 5% CO_2 and then washed twice with PBS. Fresh culture medium (2 ml) was added into each well, starting 24 hours after AAV transduction (day 0), and this was repeated daily up to day 7. Supernatant samples were collected and preserved at –80°C. After viral transduction, cell samples were also collected from each well on day 2 for extraction of genomic DNA, total RNA, and whole cellular protein for analysis.

For AAV transduction in vivo, we injected 3.0×10^{11} viral genomes of AAV-DJ-HNF4α-IRES-GFP ($n = 5$) and AAV-DJ-IRES-GFP ($n = 4$) into the tail vein. Five animals with decompensated cirrhosis that received no AAV infection were also monitored as a control group. All animals were monitored and scored for clinical changes and by laboratory tests every week until expiration or until the end of the observation period at 14 weeks after viral infection. Untreated animals ($n = 4$) and animals treated with the control AAV-GFP vector developed progressively worsening liver function and died with a mean survival of 19 days. Treated rats showed improvement in clinical parameters, INR, total bilirubin, serum albumin level, and ammonia. All were nearly at normal levels within 2 weeks of treatment and sustained those levels for at least 100 days. One animal treated with AAV-DJ-HNF4α-IRES-GFP was sacrificed 2 weeks after viral injection to estimate early transduction efficiency. Survival assessment was statistically performed by log-rank test among 3 groups ($P < 0.05$). Values represent mean ± SD. Specimens were collected following euthanasia, and samples were preserved unfixed at –80°C, embedded in paraffin after 4% PFA fixation, and embedded in OCT compound after 2% PFA fixation. Vector transduction efficiency was estimated by immune detection for GFP.

Albumin measurement. Albumin levels from hepatocyte culture supernatants were measured by ELISA according to the manufactur-

er's instructions (Bethyl Laboratories). Five hundred thousand freshly isolated viable hepatocytes were seeded into each well of a collagen-coated 6-well plate containing 2 ml DMEM/F12 and incubated overnight at 37°C in 5% CO_2. The culture medium was replaced with 2 ml of new medium every day. Collected samples were stored at –80°C prior to analysis.

CYP3A4 activity assay. Isolated cells were cultured in DMEM/F12 at a density of 0.5 million cells per well in collagen-coated 6-well plates, as described above. CYP3A4 activity was measured on day 2 of culturing, when expression following HNF4α vector transduction had peaked, using the P450-Glo CYP3A4 assay kit (Promega), according to the manufacturer's instructions. Briefly, the culture medium was exchanged with 1 ml of fresh medium (without phenol red) containing 3 μM Luciferin-IPA. After incubation for 30 minutes at 37°C, 200 μl of culture supernatant was collected from each well and transferred into luminometer tubes. Then 200 μl of Luciferin detection regent was added to each tube. The mixture was incubated for 20 minutes at room temperature and protected from light, and the luminescence was immediately detected using a TD-20/20 luminometer (Turner BioSystems Inc.).

Hepatocyte transplantation. Four-week-old male inbred Nagase analbuminemic rats (weighing approximately 100–130 g) were treated with 2 doses of 30 mg/kg retrorsine, a pyrrolizidine alkaloid that inhibits hepatocyte proliferation (43–45), given 2 weeks apart by intraperitoneal injection. Four weeks after the last injection, a 70% partial hepatectomy was performed to induce donor hepatocyte proliferation. Hepatectomy was performed by ligation of the median and left lateral lobes of the liver. Animals (5 animals per group) were then transplanted via the spleen with primary hepatocytes isolated from normal, cirrhotic rat livers or HNF4α-treated cirrhotic rat livers, or they received intrasplenic injection of 0.1 ml DMEM as a control. Cyclosporine was given to control rejection by daily intramuscular injection at 15 mg/kg body weight. Five million cells, for each transplant procedure, were washed, resuspended in 0.1 ml PBS, and injected into the splenic pulp over 30 seconds using a 27-gauge needle. Primary hepatocytes injected into the spleens of recipient non-cirrhotic rodents are known to migrate and engraft into the liver parenchyma.

Statistics. Statistical analyses were performed using the Tukey-Kramer multiple comparisons procedure using SPSS v16.0 software. Survival in vivo was evaluated by log-rank test. Each value represents the mean ± SD. Statistical analysis was performed mostly among groups that included normal hepatocytes and compensated and decompensated cirrhotic hepatocytes; and between untreated decompensated cirrhotic hepatocytes and decompensated cirrhotic hepatocytes 14 weeks after in vivo HNF4α re-expression. A P value less than 0.05 was considered statistically significant.

Study approval. All procedures performed on animals were approved by the University of Pittsburgh Animal Care and Use Committees, and thus within the guidelines for humane care of laboratory animals.

Acknowledgments

We thank A. Russell and D. Perlmutter for their comments. This work was supported by grants NIDDK R01 DK48794 (to I.J. Fox), Department of Defense (DOD) W81XWH-11-1-0803 (to I.J. Fox), NIDDK R01 DK099320 (to I.J. Fox and J. Locker), and NIDDK DK099257 (to A. Soto-Gutierrez).

Address correspondence to: Ira J. Fox, Children's Hospital of Pittsburgh, 4401 Penn Avenue, Pittsburgh, Pennsylvania 15224, USA. Phone: 412.692.7144; E-mail: foxi@upmc.edu. Or to: Alejandro Soto-Gutierrez, Department of Pathology, 200 Lothrop, S-BST, Room S-423, Pittsburgh, Pennsylvania 15213, USA. Phone: 412.648.0064; E-mail: sotogutierreza@upmc.edu.

1. Durand F, Valla D. Assessment of the prognosis of cirrhosis: Child-Pugh versus MELD. *J Hepatol*. 2005;42(suppl 1):S100–S107.
2. Gines P, Cardenas A, Arroyo V, Rodes J. Management of cirrhosis and ascites. *N Engl J Med*. 2004;350(16):1646–1654.
3. Schuppan D, Afdhal NH. Liver cirrhosis. *Lancet*. 2008;371(9615):838–851.
4. Friedman SL. Liver fibrosis — from bench to bedside. *J Hepatol*. 2003;38(suppl 1):S38–S53.
5. Martinez-Hernandez A, Martinez J. The role of capillarization in hepatic failure: studies in carbon tetrachloride-induced cirrhosis. *Hepatology*. 1991;14(5):864–874.
6. Pessayre D, Lebrec D, Descatoire V, Peignoux M, Benhamou JP. Mechanism for reduced drug clearance in patients with cirrhosis. *Gastroenterology*. 1978;74(3):566–571.
7. Vaubourdolle M, et al. Evidence of the intact hepatocyte theory in alcoholic cirrhosis. *Scand J Gastroenterol*. 1989;24(4):467–474.
8. Lopez PM, Martin P. Update on liver transplantation: indications, organ allocation, and long-term care. *Mt Sinai J Med*. 2006;73(8):1056–1066.
9. Choi J, Ou JH. Mechanisms of liver injury. III. Oxidative stress in the pathogenesis of hepatitis C virus. *Am J Physiol Gastrointest Liver Physiol*. 2006;290(5):G847–G851.
10. Kitada T, Seki S, Iwai S, Yamada T, Sakaguchi H, Wakasa K. In situ detection of oxidative DNA damage, 8-hydroxydeoxyguanosine, in chronic human liver disease. *J Hepatol*. 2001;35(5):613–618.
11. Grattagliano I, et al. Mitochondria in chronic liver disease. *Curr Drug Targets*. 2011;12(6):879–893.
12. Krahenbuhl S. Alterations in mitochondrial function and morphology in chronic liver disease: pathogenesis and potential for therapeutic intervention. *Pharmacol Ther*. 1993;60(1):1–38.
13. Liu L, et al. The microenvironment in hepatocyte regeneration and function in rats with advanced cirrhosis. *Hepatology*. 2012;55(5):1529–1539.
14. Hoare M, Das T, Alexander G. Ageing, telomeres, senescence, and liver injury. *J Hepatol*. 2010;53(5):950–961.
15. Lechel A, Manns MP, Rudolph KL. Telomeres and telomerase: new targets for the treatment of liver cirrhosis and hepatocellular carcinoma. *J Hepatol*. 2004;41(3):491–497.
16. Kobayashi N, et al. Hepatocyte transplantation in rats with decompensated cirrhosis. *Hepatology*. 2000;31(4):851–857.
17. Marro S, et al. Direct lineage conversion of terminally differentiated hepatocytes to functional neurons. *Cell Stem Cell*. 2011;9(4):374–382.
18. Takahashi K, et al. Induction of pluripotent stem cells from adult human fibroblasts by defined factors. *Cell*. 2007;131(5):861–872.
19. Berasain C, et al. Expression of Wilms' tumor suppressor in the liver with cirrhosis: relation to hepatocyte nuclear factor 4 and hepatocellular function. *Hepatology*. 2003;38(1):148–157.
20. Limaye PB, et al. Expression of specific hepatocyte and cholangiocyte transcription factors in human liver disease and embryonic development. *Lab Invest*. 2008;88(8):865–872.
21. Locker J. Transcriptional control of hepatocyte differentiation. In: Monga SP, ed. *Molecular Pathology of Liver Diseases*. New York, New York, USA: Springer; 2011:193–201.
22. Sladek FM, Seidel S. Heaptocyte nuclear factor 4a. In: McCabe TPBE, ed. *Nuclear Receptors and Genetic Disease*. London, United Kingdom: Academic Press; 2001.
23. Bolotin E, et al. Integrated approach for the identification of human hepatocyte nuclear factor 4α target genes using protein binding microarrays. *Hepatology*. 2010;51(2):642–653.
24. Nagata H, Ito M, Cai J, Edge AS, Platt JL, Fox IJ. Treatment of cirrhosis and liver failure in rats by hepatocyte xenotransplantation. *Gastroenterology*. 2003;124(2):422–431.
25. Kyrmizi I, Hatzis P, Katrakili N, Tronche F, Gonzalez FJ, Talianidis I. Plasticity and expanding complexity of the hepatic transcription factor

network during liver development. *Genes Dev*. 2006;20(16):2293–2305.
26. Odom DT, et al. Core transcriptional regulatory circuitry in human hepatocytes. *Mol Syst Biol*. 2006;2:2006.0017.
27. Hayhurst GP, Lee YH, Lambert G, Ward JM, Gonzalez FJ. Hepatocyte nuclear factor 4alpha (nuclear receptor 2A1) is essential for maintenance of hepatic gene expression and lipid homeostasis. *Mol Cell Biol*. 2001;21(4):1393–1403.
28. Parviz F, et al. Hepatocyte nuclear factor 4alpha controls the development of a hepatic epithelium and liver morphogenesis. *Nat Genet*. 2003;34(3):292–296.
29. Sladek FM, Zhong WM, Lai E, Darnell JE, Darnell JE Jr. Liver-enriched transcription factor HNF-4 is a novel member of the steroid hormone receptor superfamily. *Genes Dev*. 1990;4(12):2353–2365.
30. Gonzalez FJ. Regulation of hepatocyte nuclear factor 4 alpha-mediated transcription. *Drug Metab Pharmacokinet*. 2008;23(1):2–7.
31. Michalopoulos GK. Liver regeneration after partial hepatectomy: critical analysis of mechanistic dilemmas. *Am J Pathol*. 2010;176(1):2–13.
32. Ponnazhagan S, et al. Adeno-associated virus 2-mediated gene transfer in vivo: organ-tropism and expression of transduced sequences in mice. *Gene*. 1997;190(1):203–210.
33. Grimm D, et al. In vitro and in vivo gene therapy vector evolution via multispecies interbreeding and retargeting of adeno-associated viruses. *J Virol*. 2008;82(12):5887–5911.
34. Yue HY, et al. Hepatocyte nuclear factor 4α attenuates hepatic fibrosis in rats. *Gut*. 2010;59(2):236–246.
35. Talchai C, Xuan S, Lin HV, Sussel L, Accili D. Pancreatic β cell dedifferentiation as a mechanism of diabetic beta cell failure. *Cell*. 2012;150(6):1223–1234.
36. Nam YJ, Song K, Olson EN. Heart repair by cardiac reprogramming. *Nat Med*. 2013;19(4):413–415.
37. Bures JBO, Huston JP. Innate and motivated behavior. In: *Techniques and Basic Experiments for the Study of Brain and Behavior*. New York, New York, USA: Elsevier; 1976:37–45.
38. Berry MN, Friend DS. High-yield preparation of isolated rat liver parenchymal cells: a biochemical and fine structural study. *J Cell Biol*. 1969;43(3):506–520.
39. Seglen PO. Preparation of isolated rat liver cells. *Methods Cell Biol*. 1976;13:29–83.
40. Trapnell C, Pachter L, Salzberg SL. TopHat: discovering splice junctions with RNA-Seq. *Bioinformatics*. 2009;25(9):1105–1111.
41. Lajugie J, Bouhassira EE. GenPlay, a multipurpose genome analyzer and browser. *Bioinformatics*. 2011;27(14):1889–1893.
42. Cawthon RM. Telomere measurement by quantitative PCR. *Nucleic Acids Res*. 2002;30(10):e47.
43. Jago MV. The development of the hepatic megalocytosis of chronic pyrrolizidine alkaloid poisoning. *Am J Pathol*. 1969;56(3):405–421.
44. Laconi E, et al. Long-term, near-total liver replacement by transplantation of isolated hepatocytes in rats treated with retrorsine. *Am J Pathol*. 1998;153(1):319–329.
45. Peterson JE. Effects of the pyrrolizidine alkaloid, lasiocarpine N-oxide, on nuclear and cell division in the liver rats. *J Pathol Bacteriol*. 1965;89:153–171.